Valence-dependent sensory-rhythmic neural entrainment modulates cortico-subcortical dynamics, attention, and memory

Hoyer, R.S.[1], Bernier, M-F.[1], Martineau, L.[2,3], Lessard Bonaventure, P.[4], Labelle, C.[1], Borderie, A.[1], Blanchette, I.[1], Blumenthal, A.[5], Albouy, P.[1]

[1]CERVO Brain Research Centre, School of Psychology, Laval University, Québec, Canada
[2]Department of Specialized Medicine, Hôpital de l'Enfant-Jésus, CHU de Québec, Laval University, QC, Canada
[3]Department of Pediatrics, Centre Mère-Enfant Soleil, CHU de Québec, Laval University, Québec, Canada
[4]Department of Surgery, Division of Neurosurgery, Hôpital de l'Enfant-Jésus, CHU de Québec, Laval University, Québec, Canada
[5]Department of Psychology, School of Social & Behavioral Sciences, Marist College, New York, USA

Summary

Recent studies have shown that sensory rhythmic stimulation can enhance executive functions by synchronizing, entraining, oscillations within higher-order cortical networks. However, whether this entrainment extends to subcortical structures and shapes human behavior remains unclear. In a first experiment, we used intracranial EEG recordings in epileptic patients during a visual search task. While neutral stimulation induced moderate entrainment, we demonstrated that 5 Hz negative-valence stimulation can significantly entrain theta oscillations in a widespread task-related cortico-subcortical network, with increased synchrony in the ventral visual stream, the hippocampus, and the dorsolateral prefrontal cortex. In a second behavioral experiment in healthy individuals, visual search performance improved under both stimulation conditions, but memory for target images, assessed through an additional recognition task, was significantly enhanced after negative stimulation. These findings unravel the role of valence in modulating subcortical brain activity and behaviors through rhythmic sensory stimulation and pave the way for its further application in clinical intervention.

Results and discussion

Brain activity has the remarkable property to mimic the rhythm of environmental sensory (e.g., visual, auditory) information[1–9]. Oscillatory activity synchronizes to external rhythms[3,8] via phase-locking[2]. This entrainment, also called resonance, is not only observable in sensory cortices[5,6,9], with possible cross-modal effects[2,9], but also propagates in a supra-modal way through higher-order brain areas supporting cognitive functions such as attention[3–7,10,11] and memory[2]. However, neuroscience research on oscillatory entrainment in higher-order brain networks is still a burgeoning field, which, to blossom, awaits the illumination of the stimulation parameters leading to supra-modal entrainment[2,12]. Particularly, while entrainment in cortical higher-order networks is currently gaining increasing interest[2,10,11], it remains unknown whether subcortical activity can be entrained through external sensory rhythms and whether this entrainment shapes cognitive performance.

We used SEEG recordings in six patients with intractable epilepsy (see Supplemental Information [SI] S1) to examine cortical and subcortical entrainment by valence-specific (neutral and negative) rhythmic visual stimulation (RVS). Subsequently, we assessed the effects of RVS on attention and memory encoding in 27 healthy young adults.

Visual search is associated with sustained increased theta and gamma power in the occipital cortex

SEEG patients performed a visual search task. In visual search trials, participants identified whether four grey-shaded items all came from the same category or one differed (e.g., 3 submarines and 1 whale; STAR★Methods). All task blocks included equal proportions of No-Target (e.g., 4 submarines), Neutral-Target (e.g., 3 submarines and 1 whale), and Threatening-Target (e.g., 3 submarines and 1 shark) trials. Both living and non-living items were used as targets (Fig. 1.A). SEEG patients performed the task correctly (see SI S2)

We first investigated the sensory response associated with the visual search. Figure 1.B shows t-values in the time-frequency domain across trials of the visual search task (Morlet decomposition[13], False Discovery Rate[FDR]-corrected *t*-test vs. baseline, $p < .001$) in the right visual cortex (AAL3 atlas, -0.5 to 2 s relative to stimulus onset, STAR★Methods). This analysis revealed that the magnitude of theta (4-8 Hz) activity increases post-search onset (0-300 s period) compared to baseline, while both theta and gamma (60-120 Hz) activity persisted until target detection. This finding aligns with previous studies suggesting that theta and gamma oscillations co-occur in the visual cortex to support both early visual information processing[14,15] and sustained engagement in visual search through attention[15] and working memory[16,17].

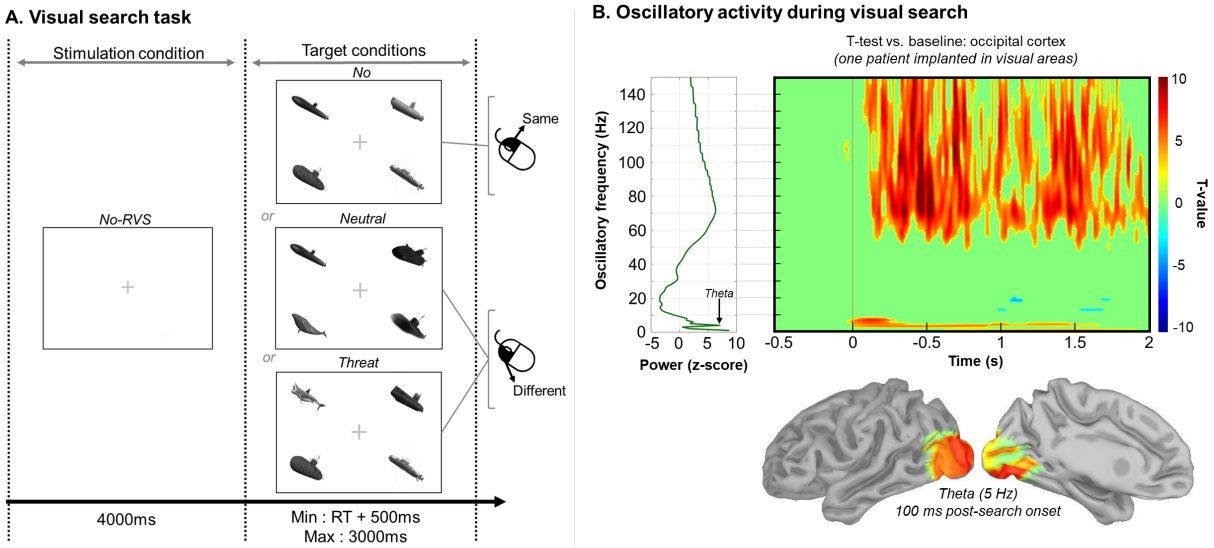

Figure 1. A) During visual search trials, participants decided if four grey-shaded items were from the same category or if one differed by pressing the right or left mouse button. Equal numbers of No-Target, Neutral-Target, and Threat-Target trials were presented. B) Left Panel: Magnitude (z-scored with baseline activity) for 0-2s period relative to stimulus onset across frequencies for SEEG contacts located in the occipital cortex. Right Panel: T values in the time frequency domain (t-test vs. baseline, FDR corrected, $p < .001$) for oscillatory activity during visual search for SEEG contacts located in the occipital cortex. The time frequency map indicates sustained theta (4-8 Hz) and gamma (60-120 Hz) activity across inferior, middle, and superior occipital gyri.

Cortico-subcortical theta power supports cognitive engagement during visual search

We next aimed to identify how theta activity propagates to brain networks to support visual search, by focusing on theta power activity, a well-established marker of inter-regional

communication during cognitive tasks[18,19]. We thus extracted Hilbert transformed magnitude of the theta band (4-8 Hz, depicted in Fig. 1.B baseline corrected with z-score) during the visual search task and during a separate Rest condition. Significant differences between task engagement and resting-state were assessed using two-tail paired *t*-tests with Monte Carlo simulations (1000) and FDR correction (all *ps* < .01) across time. To ensure the robustness of the results for identifying task-related brain network, we further employed a spatial cluster-based approach by keeping only overlapping SEEG contacts (STAR★Methods and Borderie et al., 2024[20], see also SI Tab. S3). During visual search, both early and transient (attention orienting and recognition) and late and sustained (higher-order and predictive mechanisms) processes are assumed to be involved in task execution[21–24]. Therefore, we used time series clustering approach (Dynamic Time Warping and Kmedoids, STAR★Methods) to objectively isolate theta patterns emerging during visual search (see SI Fig. S4). This analysis was performed on the difference in theta magnitude during task performance and Rest condition, over a period ranging from 0 and 1.5 s relative to search onset.

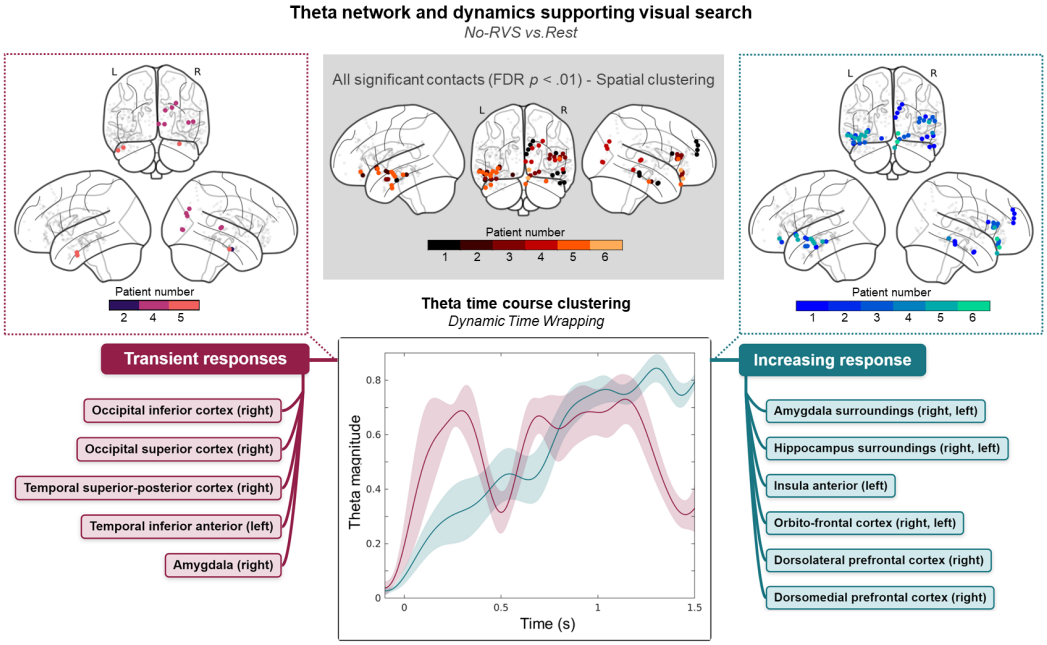

Figure 2. Spatial distribution and time courses of theta activity during visual search (-100 to 1500 ms). Middle panel: the top middle panel shows all significant SEEG contacts for the contrast task vs. rest across participants (clusters of at least two overlapping SEEG contacts). The lower middle panels show the time courses of theta activity for i) early evoked activity and later transient (purple) increase of theta oscillations for SEEG contacts located in occipital areas, the visual ventral and dorsal pathways, and the amygdala (left panel); ii) Sustained and increasing theta activity during visual search (blue line) for SEEG contacts located (MNI space) close to the amygdala and the hippocampus, the anterior insula, the orbito-frontal cortex, and the dorsolateral and dorsomedial prefrontal cortices (right panel). Shaded error bars indicate s.e.m.

As expected, spatial and temporal clustering revealed transient and sustained and increasing theta fluctuations during visual search (Fig. 2, purple and blue line, respectively). Search-onset elicited a transient theta increase followed by a late, and slightly longer response in brain regions listed in Figure 2 (in blue, left panel). These results suggest that transient activity in occipital clusters supports visual features binding[25–27], for information to be further processed along the visual dorsal ('where' stream) and ventral ('what' stream) pathways, including the superior occipital and inferior temporal cortex, respectively. Likely, visual information was

processed through theta oscillations in the superior-posterior temporal gyrus, a region involved in attention orienting[28,29]. In parallel, theta power progressively increased in the amygdala and hippocampus, reflecting ongoing associative and experience-based analysis[30–32]. The amygdala possesses strong relationships with the orbito-frontal cortex, wherein theta has been related to higher order emotional and decision processing[32–34]. Increased theta magnitude was also observed in the anterior insula, indicating focused attention and working memory[29]. Finally, an increase in theta magnitude in the dorsolateral prefrontal cortex (DLPFC), suggested mental exploration of spatial coordinates during task performance[35,36], while increase in the dorsomedial prefrontal cortex is assumed to interact with amygdala activity during fear learning[37]. These results suggest that theta oscillations in cortical and subcortical areas support both bottom-up (visual extraction and recognition, emotion and associative mechanisms) and top-down (decision making, attention, working memory and emotion regulation) processes during active visual search. Once these task-related cortico-subcortical networks had been defined, we then questioned in the same SEEG patients whether those distributed brain areas could be entrained by rhythmic sensory stimulations to ultimately shape behavior, with the hypothesis that varying the rhythmic stimulus valence will enable sub-cortical entrainment.

Theta rhythmic visual stimulations elicit entrainment in task related cortical and subcortical networks

We studied the entrainment of oscillatory neurophysiological activity induced by 5 Hz flickering visual stimuli. This RVS frequency was selected based on the results depicted in Figure 2 (sustained increase of 5 Hz-theta activity observed over the visual search period in cortical and subcortical areas), and its effectiveness in entraining cortical oscillations within the central executive network[2]. Before each trial of the visual search task, we presented 5 Hz RVS (4 s stimulation) to synchronize brain oscillatory activity and prime the task network and investigated selective entrainment by varying stimulus valence (Negative-RVS, snake stimulation; Neutral-RVS, rope stimulation – stimuli not used as target in the visual search task).

To evaluate neural entrainment, we computed the stimulation-to-brain phase-locking value (Stim-Brain PLV[38]) and investigated the phase relationship between the patients' 5 Hz ongoing oscillations and a theoretical pure 5 Hz sinusoid (reflecting rhythmic visual stimulation) over the trial time. The task period considered ranged from -4 to 0 s (stimulation period) and 0 to 2 s post-search onset (response period). This analysis was done for each trial, each SEEG contact, and for all participants. We then contrasted, for each patient, No-RVS, Neutral-RVS and Negative -RVS (Negative-RVS) using two-tail paired t-tests ($p < .05$) with Monte Carlo simulations (1000). To identify networks entrained with the 5 Hz RVS at the group level, a cluster-based method was employed: only groups of adjacent contacts (minimum: 2) exhibiting statistically significant increased Stim-Brain PLV were considered[20] (see SI S5).

This analysis revealed that PLV was significantly higher in Negative-RVS compared to both No- and Neutral-RVS during the stimulation period. In the Negative-RVS compared to No-RVS, the Stim-Brain PLV was specifically enhanced in the inferior occipital cortex (right), medial temporal gyrus (left), hippocampus and its lateral surroundings (right), anterior insula (right), and DLPFC (right, Fig. 3.B and SI S3 and S4). In Negative-RVS compared to Neutral-RVS, the PLV was increased in the medial temporal gyrus (left), hippocampus and its

surroundings, and DLPFC (right, Fig. 3.C and SI Fig.). No significant results were observed during the response period after cluster correction.

Neutral-RVS induced intermediate entrainment (no significant difference with No-RVS). 5 Hz Negative-RVS induced higher order phase-locked entrainment by non-additively priming theta activity in the visual ventral pathway (middle temporal cortex), the hippocampus and the DLPFC. This foundational evidence suggests that theta Negative-RVS can be used to effectively entrain activity across cortical and subcortical brain networks.

Based on these results, we next questioned whether such stimulation can modulate behavioral performance in a group of healthy individuals.

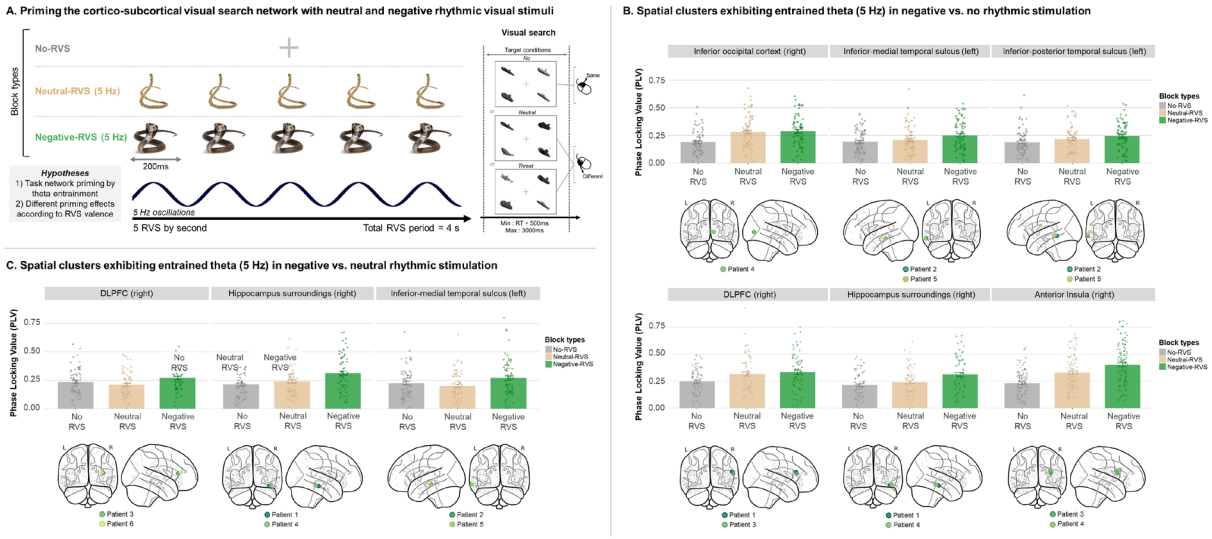

Figure 3. A) Blocks with no, neutral valence (rope), and negative valence (snake) 5 Hz RVS were used to prime the visual search network in a block design, presented before each trial. B) SEEG contacts (cluster-corrected) showing increased 5 Hz PLV in the negative valence-RVS compared to the No-RVS condition. C) SEEG contacts (cluster-corrected) showing increased 5 Hz PLV in the Negative-RVS compared to the Neutral-RVS condition. Bar plots display mean stim-brain PLV for each block type, with error bars indicating SEM and dots representing individual data points. Green dots on brain maps indicate the anatomical localization of significant clusters (paired t-tests).

Negative theta RVS boosts attention and memory in healthy adults

We conducted a behavioral experiment in 27 healthy adults (mean age: 25.9 ± 3.4 years; S6) to investigate the impact of entrainment driven by theta Neutral-RVS (Rope/Control) and Negative-RVS (Snake/Threatening) on visual search performance. In this behavioral experiment, the visual search task was identical to that performed by SEEG patients but included a recognition block (episodic memory without stimulation) instead of a rest period at the end of the visual search blocks. Participants were not instructed to memorize items during the search task to test involuntary episodic learning and memory (Fig. 1 and 4.A). The recognition block (72 trials) included visual search targets (50%) and distractors (50%). Instructions for the recognition block were given only after the completion of the visual search task.

In SEEG patients, we have shown that Negative-RVS resonance propagates across networks involved in sensory and attention processing, as well as subcortical areas including

the amygdala and the hippocampus, which play a notable role in fear learning and memory[20,31,32,37,39]. Thereby, we expected the Negative-RVS to prime the task network, boosting both attention and memory. SEEG results of Neutral-RVS indicate a transitional phase-locking stage for RVS. We therefore hypothesized either a null or a minimal impact of Neutral-RVS on performance. As we were interested in investigating possible interaction between Neutral- and Negative-RVS and visual information to be detected, the target factor (No-, Neutral- and Threatening-Target) was considered in the following analyses.

Visual search accuracy averaged 91.4 ± 0.8%, and median RT of 1228.3 ± 30.9 ms; these variables were unaffected by age, sex, or handedness (Supplemental Information). No effect of Target or RVS condition was observed on accuracy. Target condition significantly affected reaction time ($\chi^2(2) = 29.9$, $p < .001$): participants responded faster to Neutral- and Threat-Target trials than No-Target trials (both $p < .001$), with a threat superiority effect for Threat over Neutral Targets ($p < .001$). This effect was expected in healthy adults[40,41], while disregarded in SEEG analysis because of limited sample size (4 by level for Target*RVS interaction). Additionally, RT were faster in blocks with Neutral- and Negative-RVS compared to No-RVS (both $p < .001$, Fig. 4.B; RT Neutral-RV vs. Negative-RVS: $p = .276$, suggesting that theta RVS speeds up processing, irrespective of accuracy. This unspecific effect of RVS might optimize further neural framing of visual information into “perceptual moments” through theta oscillations[42,43]. This principle, also known as “theta phase precession”, is crucial for the hippocampus to encode spatial features, which in turn, enable efficient attention orienting during visual search[44]. In parallel, theta suppression in the insula has been associated with reduced arousal (physiological alertness) elicited by threat perception[45]. As we have observed in the SEEG data that 5 Hz Neutral- and Negative-RVS entrained theta in the insula (moderately and significantly, respectively, Fig. 3.B), we propose that 5 Hz RVS may prevent theta suppression by heightening arousal. This hypothesis aligns with behavioral effects observed in healthy adults, with faster responses for trials with RVS irrespective of valence.

Given the facilitating role of theta phase precession in encoding[42,43], we next sought to investigate whether the entrainment induced by theta RVS, particularly in the Negative-RVS condition, could facilitate memory encoding of target stimuli during visual search, consequently enhancing participants’ episodic memory performance in the recognition task (Fig. 4.A). In the recognition task, the mean accuracy was 58.1 ± 0.9 % (min: 51.4 %, max: 70.8 %) and the mean median RT 1207.7 ± 36.6 ms. There was no effect of Target on RT ($p = .068$). However, stimulation had a significant effect on accuracy ($\chi^2(3) = 15.8$, $p = .001$) driven by increased recognition rates of items (threat or neutral) seen in the Negative-RVS block compared to distractors ($p < .001$, Fig. 4.C; all other contrasts were non-significant, with $p = .062$ for Distractor vs. No-RVS block as closest tendency). Based on the SEEG results, we propose that this facilitation effect might ensue from the theta phase precession phenomenon, promoting memory encoding during visual search, as suggested by higher accuracy for items seen in the Negative-RVS block compared to distractors. These results can be linked to the SEEG data, where the time course of theta activity in the hippocampus and the DLPFC was classified as progressively increasing (Fig. 2) during visual search, two regions affected by significant Negative-RVS entrainment. Combining SEEG and behavioral results, we propose that Negative-RVS is likely to boost accumulation of visual evidence prior to the motor response[46] through recognition (ventral visual pathway)[47,48], and top-down attention (DLPFC) interaction with basic memory processes (hippocampus)[47–50].

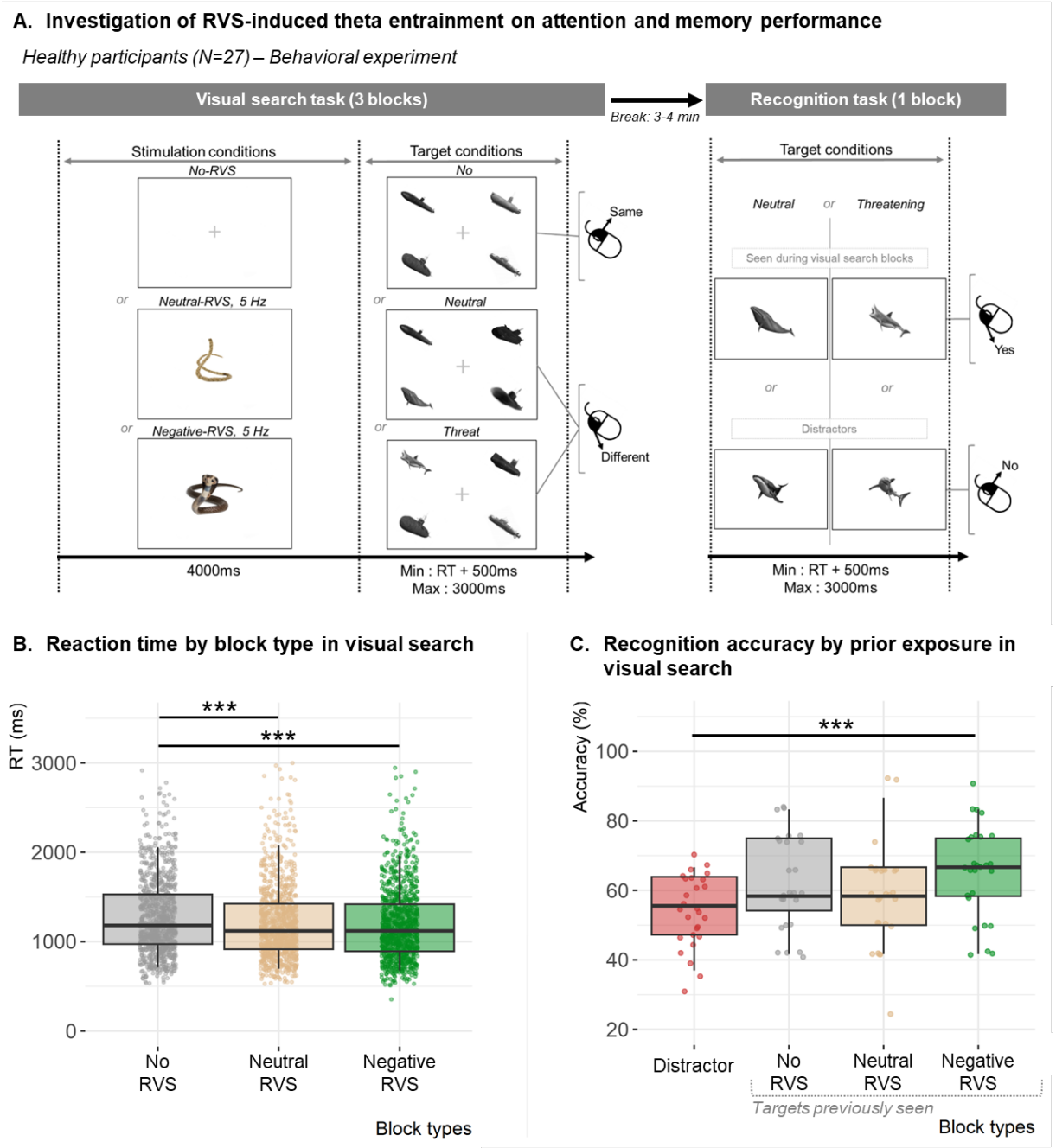

Figure 4. A) In the recognition task (right panel), participants were asked to determine whether a gray-shaded item had previously been presented as a target during the visual search blocks. Importantly, they were not informed in advance that their memory for these items would be tested. B) Median reaction time in the visual search task by stimulation conditions, and C) mean accuracy in the recognition task according to condition of prior exposure. In each boxplot, the horizontal line represents the median measure for the group, and the box shows the interquartile range. The vertical line indicates the 5th and 95th percentiles. Dots represent individual data. ***$p < .001$.

Conclusion

This study identifies distinct theta activity patterns during visual search, highlighting the interaction between transient and sustained theta oscillatory dynamics in spatial attention[21,23,24,51], advancing our understanding of neural oscillations in cognitive processes[52]. Additionally, it highlights that the emotional valence of rhythmic sensory stimulations can

significantly enhance neural entrainment in subcortical networks. While rhythmic stimulation typically engages oscillatory activity at the stimulation frequency in cortical structures, our findings demonstrate that valence can modulate this entrainment by facilitating the recruitment of subcortical regions. This suggests that valence acts as a powerful parameter to extend the influence of sensory rhythmic stimulation, optimizing the synchronization of cortico-subcortical mechanisms. By leveraging this effect, valence-driven rhythmic stimulation could provide a non-invasive means to complement deep electrical or magnetic stimulation techniques[53,54]s. Finally, amid the debate on possible distinct effects for automatic and top-down driven entrainment[12,55] (i.e., effect varying with attention paid to stimulation), these results suggest that supra-modal top-down entrainment, occurring in the spotlight of attention, can use emotional parameters to optimize synchronization to external rhythms.

STAR★Methods

Resource availability

Lead contact

Further information and data that support the findings of this study are available upon request from the corresponding author, Roxane S. Hoyer (roxane.hoyer@cervo.ulaval.ca).

Material availability

The stimuli and codes used to build and present the behavioral task are available online on OSF (https://osf.io/g4ap5/). The raw brain data used in this study (MRI and SEEG recordings) are protected as acquired through clinical assessment and are not available for sharing (2022-5890). Pre-processed SEEG data used to generate the figures and MATLAB scripts are available at the following URL.

Data and code availability

Original codes used to process SEEG and behavioral data are publicly available on OSF (https://osf.io/g4ap5/), or upon request to the corresponding author.

Experimental design and populations

Patients

SEEG data from 6 patients suffering from drug-resistant focal epilepsy were collected (mean age and standard deviation: 30 ± 3.9 years; male: 50 %, female: 50 %) following the Research Opportunities in Humans Consortium guidelines[56]. All patient performed the task appropriately. The study protocol was described verbally by the research and clinical teams and the participation was discussed prior to hospitalization with patients. All of them provided verbal assent and written informed consent. This research complies with all relevant ethical regulations; the experimental procedures were approved by the Ethics Review Board of the CHU de Québec - Université Laval (2022-5890, Québec, QC, Canada).

Healthy participants

Behavioral data from 27 neurologically healthy young adults were collected and analyzed (mean age: 25.9 ± 3.4 years; male: 52 %, female: 48 %). All participants reported normal or corrected vision and hearing, in addition to no history of neurological or psychiatric disorder. They gave written informed consent and received a monetary compensation for their participation. All participants provided verbal assent and written informed consent. This project was approved by the Ethics Review Board of the CIUSSS de la Capitale Nationale (2022-2476, Québec, QC, Canada).

Method details

Behavioral tasks

SEEG experiment. Intracranial SEEG recordings were obtained from 6 neurosurgical patients with focal drug-resistant epilepsy. In visual search trials, they viewed four items in grey shades and had to quickly determine if all items were from the same category (e.g., 4 submarines) or if one item was different (e.g., 3 submarines and 1 whale) by pressing the right or left mouse key. They had 3 s to respond before the next trial. All task blocks included equal proportions of No-Target (e.g., 4 submarines), Neutral-Target (e.g., 3 submarines and 1 whale), and Threatening-Target (e.g., 3 submarines and 1 shark) trials. Both living and non-living items were used as targets (Fig. 1.A).

In the No-RVS block, each trial was preceded by a 4 s fixation cross. In the Neutral-RVS block and Negative-RVS block, trials were preceded by a 4 s display of 5 Hz flickering picture of a rope or a snake (50 ms duration, 200 ms inter-onset interval), respectively (see Fig. 3). The negative and neutral stimuli were projected on a screen (1024*768 pixels located 50cm in front of the participant). The duration of each block (36 trials) varied as a function of participants' response time (minimum block duration: 3 min 36 s, maximum: 5 min 24 s). The task was implemented using a block design, with blocks randomization across patients. Target types and positions were balanced within and across task blocks. Once the task performed, patients' brain activity was recorded during an open-eyes resting state period (5 min 24 s). Overall, brain activity in SEEG patients was recorded across four blocks: No-RVS, Neutral valence-RVS, Negative valence-RVS, and Rest.

Patients were informed they were going to perform an attention task, including two blocks with trials preceded by flickering images before each trial. They were instructed to passively observe pictures (Rope-Neutral valence and Snake-Negative valence RVS) flickering at 5Hz before each task trial; if none were presented (No-RVS condition), they were asked to keep fixating the center of a blank screen. Participants were instructed to indicate as quickly as possible if all items belonged to the same pictorial category (right mouse button for "yes," left for "no").

Healthy participants. Healthy adults performed the exact same task and blocks as SEEG patients but the rest period was replaced by a memory-recognition block, where they were shown targets that had been presented in the visual search blocks (Neutral- and Threatening-Targets) alongside distractors (Fig. 3.A). Each trial of the recognition task began with a 2 s fixation cross, followed by a single item which participants had 3 s to determine if this item has

been previously seen or not seen during the visual search task. In 50% of the trials, the grey-shaded item, was a visual search target. We used an equal number of neutral and threatening, and living and non-living, stimuli. In the other 50%, the item was a distractor, slightly different from the visual search task targets. In the recognition block, the distractors were matched to targets' valence (neutral, threatening) and nature (living, non-living). This block was challenging, as participants were not informed beforehand that they will perform a recognition task using the targets from the visual search blocks. Participants were therefore encouraged to perform accurately but to give intuitive responses if unsure.

Procedure

SEEG patients, with electrodes implanted based on clinical requirements, were tested individually at the Hôpital de l'Enfant-Jésus, CHU de Québec (QC, Canada) in a dedicated SEEG Epilepsy Monitoring Unit. SEEG data were recorded continuously, and patients were seated approximately 50 cm from the computer screen. Prior to the recording, each patient received verbal and illustrated instructions to ensure task comprehension, without any practice trials. Presentation software (Neurobehavioral Systems, Albany, CA, USA) was used to present visual stimuli and record behavioral responses. They completed three VS blocks of 36 pseudo-randomized trials each; block order was randomized across Stimulation conditions (No-RVS, Neutral-RVS, Negative-RVS). Patients were instructed to maintain focus on the screen and respond as fast as possible using the mouse keys. After completing the VS task blocks, patients underwent a resting-state recording period.

Healthy participants were tested individually in a quiet room with the same procedure and apparatus. During the task, they seated in front of a computer (~50 cm from the screen) in a quiet room. Before performing the VS task (same procedure), participants received detailed verbal and illustrated instructions (no training). Following these blocks, healthy participants performed the recognition task immediately after the VS task.

SEEG electrodes and contacts localization

Patients' brains were stereotactically implanted with 16 to 18 semi-rigid multi-lead electrodes (AdTech, diameter: 0.8 mm). According to the clinically defined targeted structures, brain activity was recorded over SEEG contacts from of 2.0 mm wide and 3, 4, 5 or 6 mm apart. A 3D anatomical MPRAGE T1-weighted MRI (3T Siemens Trio, Siemens AG, Erlangen, Germany) was recorded pre-implantation of SEEG electrodes, with 160 sagittal slices and voxels of 1mm^3 covering the whole brain. Cortical surfaces were extracted from the T1-weighted anatomical MRI and electrodes' contacts localization was defined using the post-implantation CT scan co-registered with the pre-implantation MRI (ImaGIN toolbox, https://f-tract.eu/software/imagin/). MNI coordinates were computed using the SPM toolbox (http://www.fil.ion.ucl.ac.uk/spm/) and the SEEG contacts localization was defined based on the AAL3 atlas[57].

SEEG recordings and preprocessing

Intracranial brain activity was simultaneously recorded from SEEG contacts (sampling rate: 512 Hz) using a video-SEEG monitoring system (Natus), online referencing was performed using a contact located in white matter. The signals were bandpass filtered from 0.1 to 200 Hz during acquisition. SEEG contacts contaminated by pathological epileptic activity and environmental artifacts were rejected during preprocessing in collaboration with the clinical team. A notch filter was applied to reduce powerline contamination of the raw data (main 60 Hz, harmonics 120 and 160 Hz). To analyze brain activity before motor response to the task (mean median RT in patients: 1623 ± 112.3, minimum: 1278 and maximum: 2084), SEEG signals were epoched to consider trials extending from -4 s pre- to 2 s post-search onset (baseline: -2 to 0 s or -6 to -4s depending on further analysis to be performed). Each SEEG signal was then re-referenced to its immediate neighbor through bipolar derivations. Bipolar montage refines local specificity by eliminating signal artifacts common to adjacent contacts (e.g., 60 Hz running through wires and distant physiological artifacts) and cancel effects of distant sources whose signal is spreading to adjacent sites through volume conduction. Using this method, the estimated spatial resolution of each SEEG bipolar contact was of 3-4 mm[58]. Across patients, the brain activity was recorded over a total of 77 to 84 bipolar contacts (see SI S1).

SEEG signal processing and analyses

Signal preprocessing. SEEG data were preprocessed and visually checked to reject contacts contaminated by pathological epileptic activity or environmental artifacts. SEEG preprocessing and statistical analyses were performed using Brainstorm (http://neuroimage.usc.edu/brainstorm/)[59], FieldTrip functions (www.fieldtriptoolbox.org), and custom MATLAB codes.

Morlet wavelets. To evaluate the magnitude of task-related brain oscillatory activity during RVS, time-frequency Morlet decompositions (wavelet transform of the signal) were performed for each SEEG contact, each trial and each participant. The wavelet family was defined by (f0 /sf) = 3 with f0 ranging from 1 to 150 Hz with 1 Hz steps. Time frequency maps were normalized (z-score) according to the mean magnitude computed over the baseline period (-2 to 0 s for No-RVS vs. Rest analysis, -6 to -4s for No-RVS vs Neutral-RVS or Negative-RVS analysis). Two tailed Paired T-tests with Monte Carlo simulations (1000) and FDR correction for multiple testing over time and frequencies (alpha threshold: $p < .05$) were performed for each SEEG contact of each participant (during the response period in No-RVS vs. Rest and during the stimulation and response period in No-RVS vs Neutral-RVS or Negative-RVS).

Hilbert transform. To identify time related fluctuations of oscillatory rhythms associated with task engagement (No-RVS vs. Rest, see aforementioned analysis), we used the Hilbert transform to extract magnitude of theta oscillations (see results for rational). We first band-pass filtered the signal of each SEEG contact and each trial between 4 and 8 Hz (theta) and extracted its envelope. Hilbert data were normalized (z-score) over the baseline (-2 to 0 s for No-RVS vs. Rest). Significant differences in theta magnitude across task conditions were assessed using two-tail paired T-tests (averaged over time, 0 to 2 s, visual search period) with Monte Carlo simulations and FDR correction for multiple testing over time (alpha threshold: $p < .01$) were applied. This analysis was performed using Brainstorm Matlab toolbox.

Phase-Locking Value. We then computed the Phase Locking Value (PLV), between the patients' 5 Hz oscillations and a theoretical pure 5 Hz sinusoid over the trial period. The phase-locking value (PLV) measures the magnitude of the average phase difference between two signals represented as a unit-length complex vector[38]. By presenting 5 Hz RVS before the target occurrence in two of the three task blocks, we aimed at entraining brain oscillatory activity at this frequency to prime the task network. To test this hypothesis, we performed a two-tail paired T-test between conditions (No-RVS, Neutral-RVS, Negative-RVS; positive direction with values averaged over time) with $p < .05$ as significance threshold. This analysis was performed using the Brainstorm MATLAB toolbox. The period considered ranged from 0 to 2 s following visual search onset. A baseline period from -6 to -4 s (pre-stimulation epoch) was used for normalization in comparisons between conditions (No-RVS, Neutral-RVS, and Negative-RVS).

Spatial clustering. To identify the brain areas supporting visual search and Stim-Brain PLV the MNI coordinates of SEEG contacts showing significant effects were extracted. For all patients, significant contacts were projected over a shared standardized brain space (MNI), and a 3-dimensional sphere was projected on the MRI volume showing a significant increase in oscillatory power (radius: 4 mm). The radius size was defined based on the estimated spatial resolution associated with bipolar montage. Only clusters of at least two overlapping SEEG contacts were considered as significant for all analyses, while isolated ones were disregarded (minimization of type I error rate). This analysis was performed using custom MATLAB codes (see “data and code availability” section). Spatial clusters were named based on their location according to the AAL3 altlas in the standard ICBM32 brain. Clusters of significant contacts in the anterior and medial middle temporal gyrus were respectively named “amygdala surroundings” and “hippocampus surroundings” due to their proximity with these subcortical areas (see SI S3).

Time series clustering. To identify task-related functional networks, we analyzed theta (4–8 Hz) activity using a dynamic time warping (DTW) analysis, combined with the Partitioning Around Medoids (PAM) algorithm[60,61]. DTW computes the similarity between temporal sequences by aligning time series to minimize phase and amplitude differences, making it well-suited for capturing variations in oscillatory dynamics across regions. We used this method to group theta time series with similar temporal profiles, allowing us to identify dissociated transient and sustained patterns of activity, which may reflect the engagement of distinct functional networks. Clustering was performed using the “kmedoids” MATLAB function[62], which minimizes the sum of dissimilarities within clusters by assigning each time series to its closest medoid. This analysis was implemented using the aforementioned function and custom MATLAB codes (see “data and code availability” section).

Behavioral data analyses

SEEG patients correctly performed the task (mean accuracy ± sem – No-RVS: 83.8 ± 2.5 %; Neutral-RVS: 86.1 ± 3.0 %; Negative-RVS: 84.3 ± 5.3 %) but their performance was not analyzed due to small sample size.

In healthy participants successfully performed the task (mean accuracy ± sem – No-RVS: 91.8 ± 1.2 %; Neutral-RVS: 89.8 ± 1.2 %; Negative-RVS: 92.4 ± 1.6 %). RT (> 0 ms) from correct responses were log transformed to better fit a gaussian distribution (Shapiro-Wilk test:

W = 0.91, $p < .001$). RT and accuracy to the visual search task were modeled using lmer (RT: gaussian fitting) and glm (accuracy: binomial fitting) R[63] functions (lme4 and stats packages), respectively. Five fixed factors were considered in the analysis: Target (No, Neutral and Threatening), Block (No, Neutral- or Negative-RVS), Age (numeric vector), Biological Sex (Male and Female) and Handedness (Right or Left). Target and Block were modeled with possible interaction (variables of interest), while only the main effects of Age, Biological Sex and Handedness, were considered (between-participants variables with possible cofounding effects). Finally, Participant was used as random factor in RT analysis (lmer R function), but not in accuracy (glm R function), still to avoid overfitting issues leading to singular fit, low generalization power, and high variance in predictions. The same method was applied to analyze accuracy in the recognition task (Target levels: distractor, items seen in the Neutral-RVS block, and items seen in the Negative-RVS block). Type-II Wald tests (car package) were performed on the models. P-values were considered significant at $p < .05$. When a significant main effect or interaction was found, post-hoc Honest Significant Difference (HSD) pairwise tests were performed (emmeans package). In the case of multiple comparisons, the p-value of the Tukey HSD test was adjusted using the Tukey method for comparing multiple estimates (see also SI S6 for details on the methods used to analyze behavioral data).

Acknowledgements

This work was supported by a Post doctoral fellowship from the Fonds de Recherche du Québec – Nature et Technologies to R.S.H, a grant from Fonds de Recherche du Québec - Santé and Brain Canada Future Leaders to P.A., a grant from Réseau de Bio-Imagerie du Québec to P.A., and NSERC Discovery grant to I.B. and P.A.

Authors contribution

Conceptualization, R.S.H., I.B., A.Bl. and P.A.; Methodology, R.S.H, L.M., P.L-B., I.B., A.Bl. and P.A.; Software, R.S.H., A.Bo., L.C. and P.A.; Formal Analysis, R.S.H. and P.A.; Investigation, R.S.H., M-F.B., L.M., P.L-B., A.Bo.; Resources, L.M., P.L-B. and P.A.; Data Curation, R.S.H., M-F.B., and A.Bo.; Writing – Original Draft, R.S.H.; Writing – Review and Editing, R.S.H, M-F.B, L.M., P.L-B., C.L., A.Bo., I.B., A.Bl. and P.A.; Visualization, R.S.H., L.C.; Supervision, P.A.; Funding Acquisition, R.S.H., I.B. and P.A.

Declaration of interest

The authors declare no competing financial or non-financial interests related to the content of this research.

Inclusion and diversity

We are committed to fostering inclusive, diverse, and equitable practices in all aspects of our research, ensuring that our findings contribute to a broader understanding of human neuroscience.

Data and code availability

The material used in this study, including codes and behavioral data from healthy participants are available online (https://osf.io/g4ap5/), or upon request by contacting Roxane S. Hoyer. The raw brain data used in this study (MRI and SEEG recordings) are protected as acquired through clinical assessment and are not available for sharing (2022-5890); averaged data are available online.

References

1. Herrmann, C. S. Human EEG responses to 1–100 Hz flicker: resonance phenomena in visual cortex and their potential correlation to cognitive phenomena. *Exp Brain Res* **137**, 346–353 (2001).
2. Albouy, P., Martinez-Moreno, Z. E., Hoyer, R. S., Zatorre, R. J. & Baillet, S. Supramodality of neural entrainment: Rhythmic visual stimulation causally enhances auditory working memory performance. *Sci Adv* **8**, eabj9782 (2022).
3. Graaf, T. A. de *et al.* Alpha-Band Rhythms in Visual Task Performance: Phase-Locking by Rhythmic Sensory Stimulation. *PLOS ONE* **8**, e60035 (2013).
4. Tabarelli, D., Keitel, C., Gross, J. & Baldauf, D. Spatial attention enhances cortical tracking of quasi-rhythmic visual stimuli. *NeuroImage* **208**, 116444 (2020).
5. Jaeger, C. *et al.* Targeted rhythmic visual stimulation at individual participants' intrinsic alpha frequency causes selective increase of occipitoparietal BOLD-fMRI and EEG functional connectivity. *NeuroImage* **270**, 119981 (2023).
6. Nuttall, R. *et al.* Evoked responses to rhythmic visual stimulation vary across sources of intrinsic alpha activity in humans. *Sci Rep* **12**, 5986 (2022).
7. Lakatos, P., Karmos, G., Mehta, A. D., Ulbert, I. & Schroeder, C. E. Entrainment of neuronal oscillations as a mechanism of attentional selection. *Science* **320**, 110–113 (2008).
8. Thut, G., Schyns, P. & Gross, J. Entrainment of Perceptually Relevant Brain Oscillations by Non-Invasive Rhythmic Stimulation of the Human Brain. *Frontiers in Psychology* **2**, (2011).
9. Bauer, A.-K. R., Ede, F. van, Quinn, A. J. & Nobre, A. C. Rhythmic Modulation of Visual Perception by Continuous Rhythmic Auditory Stimulation. *J. Neurosci.* **41**, 7065–7075 (2021).
10. Pomper, U., Szaszkó, B., Pfister, S. & Ansorge, U. Cross-modal attentional effects of rhythmic sensory stimulation. *Atten Percept Psychophys* **85**, 863–878 (2023).
11. Gulbinaite, R., Viegen, T. van, Wieling, M., Cohen, M. X. & VanRullen, R. Individual Alpha Peak Frequency Predicts 10 Hz Flicker Effects on Selective Attention. *J. Neurosci.* **37**, 10173–10184 (2017).
12. Lakatos, P., Gross, J. & Thut, G. A New Unifying Account of the Roles of Neuronal Entrainment. *Current Biology* **29**, R890–R905 (2019).

13. Tallon-Baudry, C. & Bertrand, O. Oscillatory gamma activity in humans and its role in object representation. *Trends Cogn Sci* **3**, 151–162 (1999).

14. Luo, L. *et al.* Distinct roles of theta and gamma rhythms in inter-areal interaction in human visual cortex revealed by cortico-cortical evoked potentials. *Brain Stimulation: Basic, Translational, and Clinical Research in Neuromodulation* **15**, 1048–1050 (2022).

15. Spyropoulos, G., Bosman, C. A. & Fries, P. A theta rhythm in macaque visual cortex and its attentional modulation. *Proc Natl Acad Sci U S A* **115**, E5614–E5623 (2018).

16. Biel, A. L., Minarik, T. & Sauseng, P. EEG cross-frequency phase synchronization as an index of memory matching in visual search. *Neuroimage* **235**, 117971 (2021).

17. Peylo, C., Friedrich, E. V. C., Minarik, T., Biel, A. L. & Sauseng, P. Theta:gamma phase coupling and evoked gamma activity reflect the fidelity of mental templates during memory matching in visual perception. *Cereb Cortex* **32**, 4156–4171 (2022).

18. Albouy, P., Baillet, S. & Zatorre, R. J. Driving working memory with frequency-tuned noninvasive brain stimulation. *Ann N Y Acad Sci* (2018) doi:10.1111/nyas.13664.

19. Albouy, P., Weiss, A., Baillet, S. & Zatorre, R. J. Selective Entrainment of Theta Oscillations in the Dorsal Stream Causally Enhances Auditory Working Memory Performance. *Neuron* **94**, 193-206.e5 (2017).

20. Borderie, A. *et al.* Cross-frequency coupling in cortico-hippocampal networks supports the maintenance of sequential auditory information in short-term memory. *PLoS Biol* **22**, e3002512 (2024).

21. Bonnefond, M., Jensen, O. & Clausner, T. Visual Processing by Hierarchical and Dynamic Multiplexing. *eNeuro* **11**, (2024).

22. Dugué, L., Marque, P. & VanRullen, R. Theta Oscillations Modulate Attentional Search Performance Periodically. *Journal of Cognitive Neuroscience* **27**, 945–958 (2015).

23. Johnson, E. L. *et al.* A rapid theta network mechanism for flexible information encoding. *Nat Commun* **14**, 2872 (2023).

24. Su, M. *et al.* Theta Oscillations Support Prefrontal-hippocampal Interactions in Sequential Working Memory. *Neurosci. Bull.* **40**, 147–156 (2024).

25. Ghiani, A., Maniglia, M., Battaglini, L., Melcher, D. & Ronconi, L. Binding Mechanisms in Visual Perception and Their Link With Neural Oscillations: A Review of Evidence From tACS. *Front Psychol* **12**, 643677 (2021).

26. Klimesch, W. Binding principles in the theta frequency range. in *Handbook of Binding and Memory: Perspectives from Cognitive Neuroscience* (eds. Zimmer, H., Mecklinger, A. & Lindenberger, U.) 0 (Oxford University Press, 2006). doi:10.1093/acprof:oso/9780198529675.003.0005.

27. Nakayama, R. & Motoyoshi, I. Theta-cyclic binding of visual features. *Journal of Vision* **18**, 964 (2018).

28. Cazzoli, D. *et al.* Theta burst stimulation improves overt visual search in spatial neglect independently of attentional load. *Cortex* **73**, 317–329 (2015).

29. Ramezanpour, H. & Fallah, M. The role of temporal cortex in the control of attention. *Curr Res Neurobiol* **3**, 100038 (2022).

30. Tang, A. M. *et al.* Amygdaloid theta-band power increases during conflict processing in humans. *Journal of Clinical Neuroscience* **91**, 183–192 (2021).

31. Zheng, J. *et al.* Multiplexing of Theta and Alpha Rhythms in the Amygdala-Hippocampal Circuit Supports Pattern Separation of Emotional Information. *Neuron* **102**, 887-898.e5 (2019).

32. Manssuer, L. *et al.* Integrated Amygdala, Orbitofrontal and Hippocampal Contributions to Reward and Loss Coding Revealed with Human Intracranial EEG. *J. Neurosci.* **42**, 2756–2771 (2022).

33. Llorens, A. *et al.* Decision and response monitoring during working memory are sequentially represented in the human insula. *iScience* **26**, (2023).

34. Dymond, S. *et al.* Almost winning: Induced MEG theta power in insula and orbitofrontal cortex increases during gambling near-misses and is associated with BOLD signal and gambling severity. *NeuroImage* **91**, 210–219 (2014).

35. Barbey, A. K., Koenigs, M. & Grafman, J. Dorsolateral Prefrontal Contributions to Human Working Memory. *Cortex* **49**, 1195–1205 (2013).

36. Tian, Y., Tan, C., Tan, J., Yang, L. & Tang, Y. Top-down modulation of DLPFC in visual search: a study based on fMRI and TMS. *Cerebral Cortex* **34**, bhad540 (2024).

37. Chen, S. *et al.* Theta oscillations synchronize human medial prefrontal cortex and amygdala during fear learning. *Science Advances* **7**, eabf4198 (2021).

38. Lachaux, J. P., Rodriguez, E., Martinerie, J. & Varela, F. J. Measuring phase synchrony in brain signals. *Hum Brain Mapp* **8**, 194–208 (1999).

39. Manssuer, L. *et al.* Reward recalibrates rule representations in human amygdala and hippocampus intracranial recordings. *Nat Commun* **15**, 9518 (2024).

40. Blanchette, I. Snakes, spiders, guns, and syringes: how specific are evolutionary constraints on the detection of threatening stimuli? *Q J Exp Psychol (Hove)* **59**, 1484–1504 (2006).

41. Cinq-Mars, J., Blumenthal, A., Grund, A., Hétu, S. & Blanchette, I. DLPFC controls the rapid neural response to visual threat: An ERP and rTMS study. *Brain Research* **1784**, 147850 (2022).

42. Busch, N. A., Dubois, J. & VanRullen, R. The Phase of Ongoing EEG Oscillations Predicts Visual Perception. *J. Neurosci.* **29**, 7869–7876 (2009).

43. Dragoi, G. & Buzsáki, G. Temporal encoding of place sequences by hippocampal cell assemblies. *Neuron* **50**, 145–157 (2006).

44. Kragel, J. E. *et al.* Hippocampal theta coordinates memory processing during visual exploration. *eLife* **9**, e52108.

45. Yilmaz Balban, M. *et al.* Human Responses to Visually Evoked Threat. *Curr Biol* **31**, 601-612.e3 (2021).

46. Olivers, C. N. L. & Roelfsema, P. R. Attention for action in visual working memory. *Cortex* **131**, 179–194 (2020).

47. Numan, R. A Prefrontal-Hippocampal Comparator for Goal-Directed Behavior: The Intentional Self and Episodic Memory. *Front. Behav. Neurosci.* **9**, (2015).

48. Anderson, K. L., Rajagovindan, R., Ghacibeh, G. A., Meador, K. J. & Ding, M. Theta Oscillations Mediate Interaction between Prefrontal Cortex and Medial Temporal Lobe in Human Memory. *Cerebral Cortex* **20**, 1604–1612 (2010).

49. Backus, A. R., Schoffelen, J.-M., Szebényi, S., Hanslmayr, S. & Doeller, C. F. Hippocampal-Prefrontal Theta Oscillations Support Memory Integration. *Current Biology* **26**, 450–457 (2016).

50. Hsieh, L.-T. & Ranganath, C. Frontal midline theta oscillations during working memory maintenance and episodic encoding and retrieval. *NeuroImage* **85**, 721–729 (2014).

51. Dugué, L., Marque, P. & VanRullen, R. Theta Oscillations Modulate Attentional Search Performance Periodically. *Journal of Cognitive Neuroscience* **27**, 945–958 (2015).

52. Doelling, K. B. & Assaneo, M. F. Neural oscillations are a start toward understanding brain activity rather than the end. *PLoS Biol* **19**, e3001234 (2021).

53. Liu, X., Qiu, F., Hou, L. & Wang, X. Review of Noninvasive or Minimally Invasive Deep Brain Stimulation. *Front Behav Neurosci* **15**, 820017 (2022).

54. Lozano, A. M. *et al.* Deep brain stimulation: current challenges and future directions. *Nat Rev Neurol* **15**, 148–160 (2019).

55. Bouwer, F. L. Neural Entrainment to Auditory Rhythms: Automatic or Top-Down Driven? *J. Neurosci.* **42**, 2146–2148 (2022).

56. Feinsinger, A. *et al.* Ethical commitments, principles, and practices guiding intracranial neuroscientific research in humans. *Neuron* **110**, 188–194 (2022).

57. Tzourio-Mazoyer, N. *et al.* Automated anatomical labeling of activations in SPM using a macroscopic anatomical parcellation of the MNI MRI single-subject brain. *Neuroimage* **15**, 273–289 (2002).

58. Jerbi, K. *et al.* Exploring the electrophysiological correlates of the default-mode network with intracerebral EEG. *Front Syst Neurosci* **4**, 27 (2010).

59. Tadel, F., Baillet, S., Mosher, J. C., Pantazis, D. & Leahy, R. M. Brainstorm: a user-friendly application for MEG/EEG analysis. *Comput Intell Neurosci* **2011**, 879716 (2011).

60. Park, H.-S. & Jun, C.-H. A simple and fast algorithm for K-medoids clustering. *Expert Systems with Applications* **36**, 3336–3341 (2009).

61. Kaufman, L. & Rousseeuw, P. *Finding Groups in Data: An Introduction To Cluster Analysis*. *Wiley, New York. ISBN 0-471-87876-6.* (1990). doi:10.2307/2532178.

62. Bache, K. & Lichman, M. UCI Machine Learning Repository. *School of Information and Computer Sciences, University of California, Irvine.* (2013).

63. R Foundation for Statistical Computing. R: A language and environment for statistical computing. (2021).